Tikrit Journal of Engineering Sciences (2025); 32(3): 1485
DOI: http://doi.org/10.25130/tjes.32.3.3

IRAQI Academic Scientific Journals

ISSN: 1813-162X (Print); 2312-7589 (Online)
Tikrit Journal of Engineering Sciences
available online at: http://www.tj-es.com

TJES Tikrit Journal of Engineering Sciences

Dynamic Stiffness and Damping of Rigid Retaining Wall under Seismic Loading

Mohammed N. Jaro *, Ahmed I. Mohammed
Civil Engineering Department, College of Engineering, University of Mosul, Mosul, Iraq.

Keywords:
Backfill soil; Dimensionless frequency; Dynamic damping; Dynamic stiffness; Rigid retaining wall.

Highlights:

- *Dynamic stiffness and damping of the soil under the base of the retaining wall.*
- *Dynamic stiffness and damping of the backfill soil behind the retaining wall.*
- *Dynamic sliding damping and dynamic rocking damping of backfill soil behind the retaining wall.*

ARTICLE INFO
Article history:

Received	05 Aug.	2023
Received in revised form	28 Oct.	2023
Accepted	10 Aug.	2024
Final Proofreading	26 Jan.	2025
Available online	17 June	2025

Citation: Jaro MN, Mohammed AI. **Dynamic Stiffness and Damping of Rigid Retaining Wall under Seismic Loading**. *Tikrit Journal of Engineering Sciences* 2025; **32**(3): 1485.
http://doi.org/10.25130/tjes.32.3.3

**Corresponding author:*
Mohammed N. Jaro
Civil Engineering Department, College of Engineering, University of Mosul, Mosul, Iraq.

Abstract: Dynamic stiffness and damping of the soil under the base of the foundation of the retaining wall and the backfill soil behind it play the main role in estimating vibrating displacement during seismic loading. The purpose of the present study is to investigate the effect of dimensionless frequency (a_o) on the horizontal, vertical, and rocking dynamic stiffness and dynamic damping of rigid retaining walls. On the other hand, the effect of (a_o) and height of the retaining wall on the stiffness and damping for backfill soil behind the rigid retaining wall was also investigated in the cases of active and passive dynamic sliding and dynamic rocking. The study demonstrated that the dynamic stiffness and damping of the soil under the base of the rigid retaining wall increased with the soil shear modulus. While the dynamic stiffness and damping of the backfill soil behind the retaining wall increased with the wall height. The percentage of increment generally varied between (42.1 – 113.2)% when the height of the retaining wall rose from (4 to 6) m. The maximum horizontal, rocking, and vertical dynamic stiffness of the soil under the base of the foundation of the retaining wall occurred at high, low, and intermediate values of (a_o), respectively, i.e., at high, low, and intermediate values of angular frequencies (ω) for constant values of soil properties and retaining wall height. It can be also noted that the values of dynamic sliding damping and dynamic rocking damping of the backfill soil decreased and increased with increasing the (a_o) or (ω), respectively. The percentages of decrement and increment were (37.5)% and (183.3)% when (ao) increased from (0.19 to 1.35), respectively.

الصلابة والتخميد الديناميكيين للجدران الساندة الجاسئة تحت الاحمال الزلزالية

محمد ناظم جارو، أحمد إبراهيم محمد
قسم الهندسة المدنية/ كلية الهندسة / جامعة الموصل / الموصل – العراق.

الخلاصة

ان كلاً من الصلابة والتخميد الديناميكيين للتربة تحت أسس الجدران الساندة وكذلك تربة الردم الواقعة خلف هذه الجدران الساندة تلعبان دورًا رئيسًا في حساب الازاحة الاهتزازية اثناء التحميل الزلزالي. إن الهدف الرئيس من هذا البحث هو دراسة تأثير التردد اللابعدي (a_o) على الصلابة الديناميكية والتخميد الديناميكي للجدران الساندة الجاسئة بالاتجاهات الافقية والعمودية وكذلك الدورانية. من جهة أخرى فقد تم في هذا البحث دراسة تأثير التردد اللابعدي (a_o) إضافة الى ارتفاع الجدران الساندة على الصلابة الديناميكية والتخميد الديناميكي في الحالتين الفعالة والسلبية لوضع الزحف ووضع الدوران للتربة الواقعة خلف الجدران الساندة الجاسئة. أظهرت الدراسة ازدياد كل من الصلابة والتخميد الديناميكيين للتربة الواقعة تحت أسس الجدران الساندة الجاسئة مع زيادة معامل القص للتربة، اما بالنسبة لتربة الردم الواقعة خلف الجدران الساندة فان الصلابة والتخميد الديناميكيين يتزايدان مع زيادة ارتفاع الجدران الساندة. بصورة عامة فإن الزيادة تراوحت بين (٤٢,١ – ١١٣,٢)% عندما يزداد ارتفاع الجدار الساند من (٤ - ٦)م. إن أعظم صلابة افقية ودورانية وعمودية تحدث عند أعلى وأخفض ومتوسط قيم للتردد اللابعدي (a_o) على الترتيب، أي عند أعلى أخفض ومتوسط قيم للتردد الدوراني (ω) لقيم ثابتة لخواص التربة وابعاد الجدار الساند. كما يمكن ملاحظة أن قيمة التخميد الديناميكي لحالتي الزحف والدوران للتربة الواقعة خلف الجدران الساندة تقل وتزداد على الترتيب مع زيادة (a_o) أو (ω). إن نسبة الزيادة والنقصان كانت (٣٧,٥)% و (١٨٣,٣)% على الترتيب عندما تزداد قيمة (a_o) من (٠,١٩ إلى ١,٣٥).

الكلمات الدالة: تربة الردم، التردد اللابعدي، التخميد الديناميكي، الصلابة الديناميكية، جدار ساند جاسئ.

1.INTRODUCTION

A gravity retaining wall is thick, heavy, and stiff enough that does not bend under external loading. In the seismic area, additional loading affects the retaining wall due to the dynamic loading of the earthquake caused by increasing horizontal stress [1]. As a result, the action of the earthquake creates an effective dynamic interaction between the wall and the backfill soil. The movement of the gravity retaining wall occurs either by sliding or rotation. Retaining walls under seismic loading behave differently from those under machine foundations. This difference is because the retaining wall is embedded from one side; therefore, the movement during an earthquake will be big away from the backfill compared with this towards the backfill [2]. In the seismic area, earthquakes induce large force acting on retaining walls due to backfill relative movement. Similar to static analysis, there are two forms of pressure produced in backfill during earthquake loading: Active earth pressure, which occurs when the movement of the retaining wall is a way from the backfill, and passive earth pressure occuring when the retaining wall moves toward the backfill [3]. On the other hand, the active and passive pressure movement of the retaining wall away from the backfill and towards it will generate a friction force and will resist the motion, creating a force, known as damping and acts actively and passively according to the motion of the retaining wall with regard to the soil backfill. Soil damping can be divided into two categories: Geometrical damping and material damping. Geometrical damping, which is also called radiation damping, is created due to the propagation of a wave through an elastic medium. This type of damping is a function of distance to the source of the wave. Material damping expresses the energy dissipation through the medium by hysteresis. Material damping is a function of stress level that develops during dynamic loading, such as earthquakes, and produces a hysteretic stress-strain relationship. In tall structures where the horizontal and rocking mode plays the main role, material damping plays a secondary role and may be neglected [4]. Over the years, several methods have been suggested, developed, and adopted to estimate the dynamic damping and stiffness of foundations generally. Gazetas [5] studied the effect of the foundation's geometrical shape and embedment of the foundation on the dynamic damping and stiffness under oscillation frequencies. Mita and Luco [6] prepared tables of dimensionless impedance functions using the finite element method. They estimated the dynamic stiffness for many types of embedded foundations and high values of dimensionless frequency (ao) up to (3.0). Bertha et al. [7] conducted a series of expressions for the damping and natural frequencies of rigid foundations subjected to vertical and coupled horizontal-rocking harmonic dynamic loading. The formulas were obtained using the approximate expressions for the dynamic stiffness suggested by Veletsos [8, 9]. They concluded that for the horizontal-rocking case, the expressions were a function of the mass ratio, in addition to the ratio of the height of the foundation to its equivalent radius. While for the vertical case, the expressions depended on the mass ratio only [7]. The aim of the present research is to study the effect of dimensionless frequency (ao) on the horizontal, vertical, and rocking dynamic stiffness and dynamic damping of rigid retaining walls. On the other hand, the effect of (ao) and height of the retaining wall on the stiffness and damping for backfill soil behind the rigid retaining wall was also investigated in the cases of active and passive dynamic sliding and dynamic rocking.

2.METHODOLOGY

In this research, the dynamic stiffness and damping parameters of the rigid retaining wall under dynamic (seismic) loading were studied.

The effect of dimensionless frequency (a_o) and type of soil on the horizontal, vertical, and rocking dynamic stiffness and damping was investigated for the soil under the retaining wall. On the other hand, the effect of dimensionless frequency (a_o) and height of the retaining wall on the active and passive dynamic sliding and rocking stiffness and damping for backfill soil behind the retaining wall was also investigated. The static stiffness for base soil was suggested by Dobry and Gazetas [10], as illustrated below:

1- Static horizontal stiffness:

$$K_x = S_x \frac{G}{2-\mu} \quad (1)$$

where:

G: Shear modulus of the soil under the retaining wall (kN/m²).

μ: Possions ratio of the soil under the retaining wall.

S_x: Dimensionless static horizontal stiffness parameter.

The value of (S_x) for rectangular foundation of dimensions(2L, 2B) is given as:

$$S_x = 2 + 2.5 \left[\frac{B}{2}\right]^{-0.85} \quad (2)$$

However, for strip footing (the case of the base of the retaining wall), the value of Sx is equal to 2.0.

2- Static vertical stiffness:

$$K_z = S_z \frac{G}{1-\mu} \quad (3)$$

Sz: Dimensionless static vertical stiffness parameter.

$$S_z = 0.73 + 1.54 \left[\frac{B}{L}\right]^{0.75}, \text{ for } \frac{B}{L} > 0.02 \quad (4)$$

$$S_z = 0.8 \text{ , for } \frac{B}{L} < 0.02 \quad (5)$$

The value of (0.8) was taken in the case of the base of the retaining wall [10].

3- Static rocking stiffness:

$$K_\theta = \frac{\pi G B^2}{2(1-\mu)} \left(1 + \left[\frac{\ln(3-4\mu)}{\pi}\right]^2\right) \quad (6)$$

B: half of the footing width (m).

Now, the dynamic horizontal, vertical, and rocking stiffness ($K_{dyn.}$) can be calculated by multiplying the certain value of stiffness by the dimensionless stiffness coefficient ($\tilde{K}$) [11].

$$\mathbf{Kdyn} = \tilde{K}.K \quad (7)$$

Figures 1-3 show the variation of horizontal, vertical, and rocking coefficient of dynamic stiffness with dimensionless frequency (a_o).

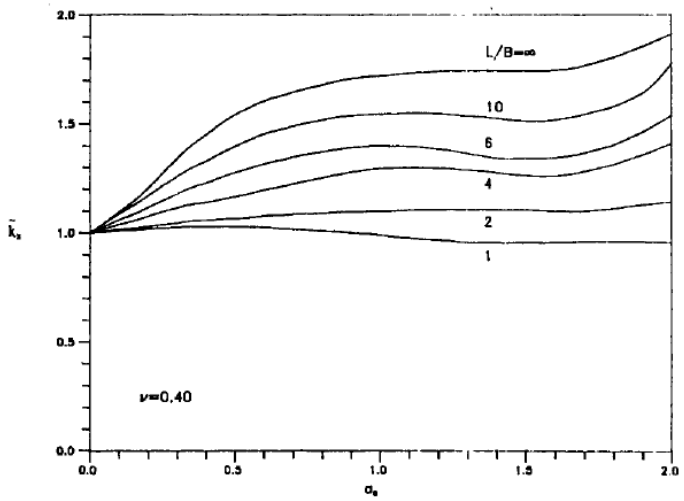

Fig. 1 The Horizontal Stiffness Coefficient Versus Dimensionless Frequency (a_o) (After Gazetas and Tassoulas) [12].

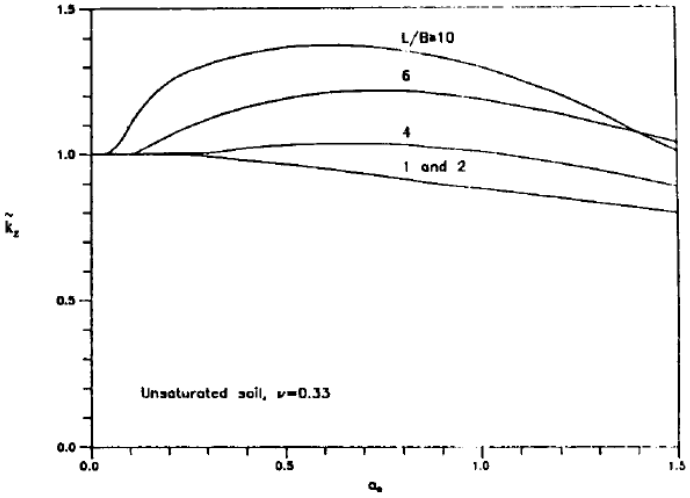

Fig. 2 The Vertical Stiffness Coefficient Versus Dimensionless Requency (a_o) (After Dobry and Gazetas) [10].

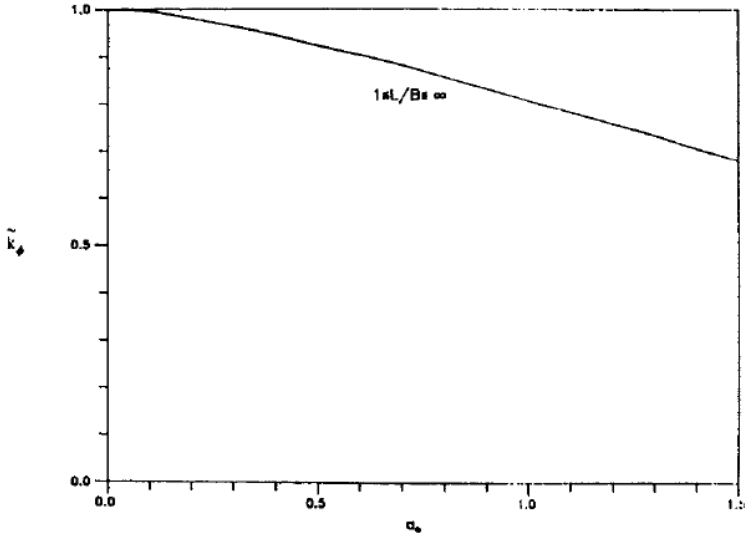

Fig. 3 The Rocking Stiffness Coefficient Versus Dimensionless Frequency (a_o) (After Dobry and Gazetas) [10].

The dimensionless frequency (a_o) for the soil under the base of the retaining wall can be defined as:

$$a_o = \omega B/v_s = \omega B\sqrt{\frac{\rho}{G}} \quad (8)$$

where:

ρ: The density of soil under the base of the retaining wall (gm/cm^3),

ω: The angular frequency, (rad/s).

It can be seen from Eq. (8) that for certain soil and geometrical dimensions of the retaining wall, i.e., for constant values of ρ, G, and B, the dimensionless frequency (a_o) is a function of angular frequency (ω). The static damping for the soil under the base of the retaining wall was also suggested by Dobry and Gazetas [10] as follows:

1- Static horizontal damping:

$$C_x = 2B\sqrt{G.\rho} \quad (9)$$

2- Static vertical damping:

$$C_z = 3.4\,(2B).Q.\sqrt{G.\rho}/\pi(1-\mu) \quad (10)$$

3- Static rocking damping:

$$C_\theta = \frac{\rho.V_{la}(2B)^3}{2(1-\mu)} \quad (11)$$

$$V_{la} = \frac{3.4}{\pi(1-\mu)}\sqrt{\frac{G}{\rho}} \quad (12)$$

Similarly to the dynamic stiffness, the dynamic horizontal, vertical, and rocking damping ($C_{dyn.}$) can be calculated by multiplying the certain value of damping calculated above by the dimensionless damping coefficient ($\tilde{C}$).

$$\mathbf{Cdyn.} = \tilde{C}\,.\,C \quad (13)$$

As previously indicated, in tall structures, such as retaining walls, the material damping plays a secondary role and can be neglected. The coefficients of geometrical damping only were determined by Dobry and Gazetas (1986). Figures 4-6 show the variation of horizontal, vertical, and rocking damping coefficients with dimensionless frequency (a_o).

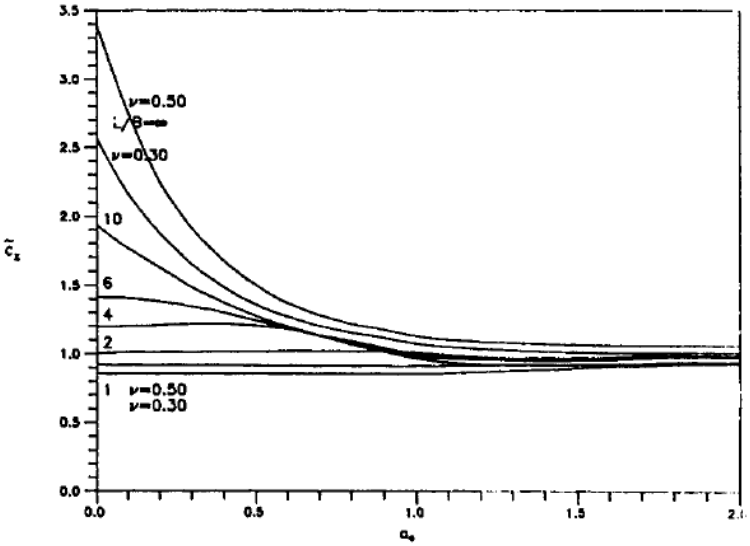

Fig. 4 The Horizontal Geometrical Damping Coefficient Versus Dimensionless Frequency (a_o) (After Gazetas and Tassoulas) [13].

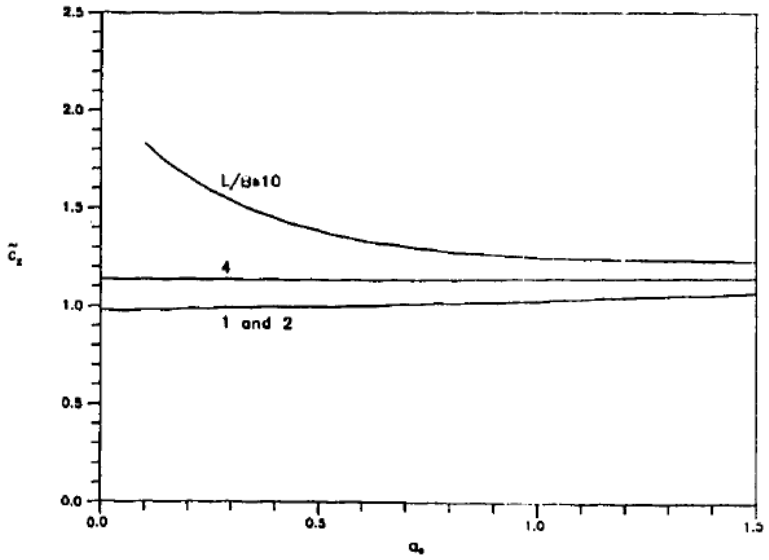

Fig. 5 The Vertical Geometrical Damping Coefficient Versus Dimensionless Frequency (a_o) (After Dobry and Gazetas) [10].

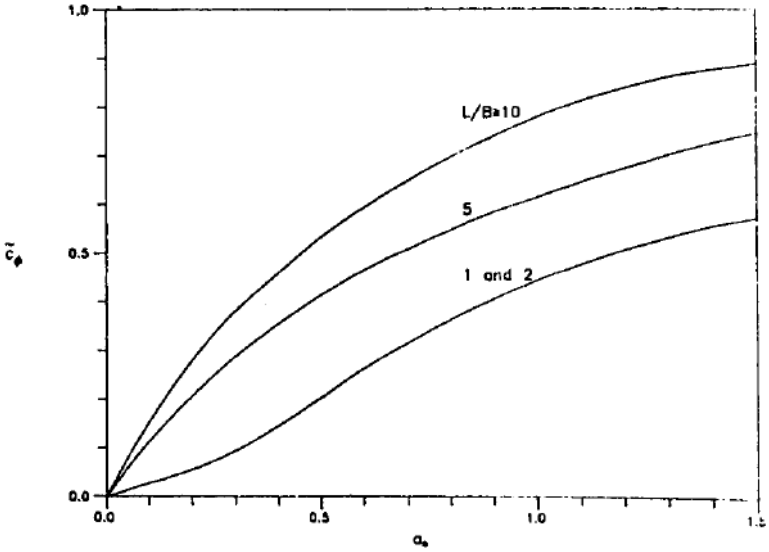

Fig. 6 The Rocking Geometrical Damping Coefficient Versus Dimensionless Frequency (a_o) (After Dobry and Gazetas) [10].

3.DYNAMIC STIFFNESS AND DAMPING OF BACKFILL MATERIAL BEHIND THE RETAINING WALL

The static stiffness or spring constant of the soil can be defined by Das and Ramana [14] as follows:

$$K = \frac{W}{Z_s} \quad (14)$$

where:
W: Load
Z_s: Static deflection
For the backfill material behind the gravity retaining wall, the static stiffness is defined as the force change to displacement change ratio. This backfill's static stiffness can be either active or passive depending on how the retaining wall moves; i.e., toward or away from the backfill.

$$K_a = \frac{P_o - P_a}{d_a} \quad (15)$$

And

$$K_p = \frac{P_p - P_o}{d_p} \quad (16)$$

where:
K_a: Active static stiffness of the backfill, (kN/m),
K_p: passive static stiffness of the backfill, (kN/m).
Nandakumaran [15] suggested the following values of d_a and d_p.

$$d_a = \frac{0.5}{100}H \quad , \quad d_p = \frac{5}{100}H$$

where:
H: The height of the retaining wall (m),
P_a: Active force (kN).

$$P_a = \frac{1}{2}\gamma H^2 \frac{\cos^2(\emptyset-\alpha)}{\cos^2\alpha.\cos(\delta+\alpha)\left[1+\sqrt{\frac{\sin(\emptyset+\delta).\sin(\emptyset-i)}{\cos(\alpha-i).\cos(\delta+\alpha)}}\right]^2} \quad (17)$$

P_p: Passive force (kN).

$$P_p = \frac{1}{2}\gamma H^2 \frac{\cos^2(\emptyset+\alpha)}{\cos^2\alpha.\cos(\delta-\alpha)\left[1+\sqrt{\frac{\sin(\emptyset+\delta).\sin(\emptyset+i)}{\cos(i-\alpha).\cos(\delta-\alpha)}}\right]^2} \quad (18)$$

P_o: Lateral force at rest, (kN).

$$P_o = \frac{1}{2}\gamma H^2.K_o \quad (19)$$

where:

γ: The unit weight of backfill soil.

δ: The friction of soil-wall (°),

α: The inclined angle of the backfill of the retaining wall (°),

Φ: The friction of the backfill soil (°),

i: The backfill surface slope (°).

Dobry and Gazetas [10] assumed that the horizontal dynamic stiffness to be valid for the backfill in the same manner as the soil under the retaining wall. The dynamic stiffness is determined by Rafnsson and Prakash [2].

$$\bar{K}_a = \tilde{K}_z.K_a \quad (20)$$

$$\bar{K}_p = \frac{K_p}{\bar{K}_z} \quad (21)$$

$$\bar{K}_{a\theta} = \tilde{K}_\theta.K_{a\theta} \quad (22)$$

$$\bar{K}_{p\theta} = \tilde{K}_\theta.K_{p\theta} \quad (23)$$

$$K_{a\theta} = K_a.h \quad (24)$$

$$K_{p\theta} = K_p.h \quad (25)$$

where;

$\bar{K}_a$: Dynamic active sliding (horizontal) stiffness(kN/m),

$\bar{K}_p$: Dynamic passive sliding (horizontal) stiffness (kN/m),

$\bar{K}_{a\theta}$: Dynamic active rocking stiffness (kN/m),

$\bar{K}_{p\theta}$: Dynamic passive rocking stiffness (kN/m).

h: The arm of the moment from the point of dynamic force acting on the backfill to the base of the wall, considered as (0.5 H) [2].

$\tilde{K}_z$ and $\tilde{K}_\theta$ from Figs. (1) and (3), respectively. The geometrical damping due to sliding and rocking is expressed as:

$$\bar{C}_x = \tilde{C}_x.K[\frac{3.4\,(2B).H.\sqrt{G.\rho}}{\pi(1-\mu)}] \quad (26)$$

$$\bar{C}_\theta = \tilde{C}_\theta[\frac{\rho.V_{la}.(2B)^3}{12}] \quad (27)$$

$$V_{la} = \frac{3.4}{\pi(1-\mu)}\sqrt{\frac{G}{\rho}} \quad (28)$$

where:

$\bar{C}_x$: dynamic geometrical damping due to sliding, (kN.s/m).

$\bar{C}_\theta$: dynamic geometrical damping due to rocking, (kN.s/m).

$\tilde{C}_x$ and $\tilde{C}_\theta$ from Figs. (4) and (6).

K: The reduction factor due to (partial half space) behavior of the retaining wall, was considered as 0.5.

4.SOIL PROPERTIES AND RETAINING WALL GEOMETRY

To study the effect of soil strength on the dynamic stiffness and damping of the soil under the base of the retaining wall, three types of soil were considered soft, stiff, and hard cohesive soil. Table 1 shows soil properties for cohesive soil under the base of the retaining wall and for cohesionless soil behind it [16]. The Poisson's ratio of the soil under the base of the retaining wall was considered as a constant value of (υ=0.4). In addition, three heights of the retaining wall were considered. Table 2 shows the geometrical characteristics of the retaining wall.

Table 1 Soil Properties for Cohesive Soil under the Base of the Retaining Wall and for Cohesionless Soil Behind it [16].

Soil type		Cohesion(c) (kN/m²)	Friction(Φ) (°)	Density(ρ) (gm/cm³)	Shear modulus G(kN/m²)
Cohesive	Soft	---	---	1.2	8000
	Stiff	---	---	1.5	12000
	Hard	---	---	1.8	20000
Cohesionless (Backfill soil)		(°)	30	1.5	

Table 2 Geometrical Characteristics of Retaining Wall [16].

R.W Height (m)	δ (°)	α (°)	i (°)
4, 5, and 6	20	2	0

5.RESULTS AND DISCUSSION

Figures 7-9 show the variation of each of the horizontal, vertical, and rocking dynamic stiffness of the soil under the base of the retaining wall with dimensionless frequency (a_o) for soft, stiff, and hard soils, respectively. Intuitively, the dynamic stiffness of the base under the retaining wall increased with the soil hardness due to increasing the soil shear modulus (G). It can be seen that the shapes of the curves in Figs. 7-9 differ from each other for horizontal, vertical, and rocking dynamic stiffness, respectively. This difference is due to the nature of the variation of dynamic stiffness coefficient with dimensionless frequency (a_o), see Figs. 1-3 for horizontal, vertical, and rocking stiffness coefficients, respectively. Generally, the maximum horizontal dynamic stiffness occurred at a high value of dimensionless frequency (a_o), i.e., at a high value of angular frequency (ω) for constant soil properties (ρ and G) and constant wall geometry (B), see Eq. (8). On the other hand, the maximum rocking dynamic stiffness occurred at a low value of dimensionless frequency (a_o), i.e., at a low value of angular frequency (ω). The maximum vertical dynamic stiffness occurred at the middle zone of the values of (a_o) and (ω).

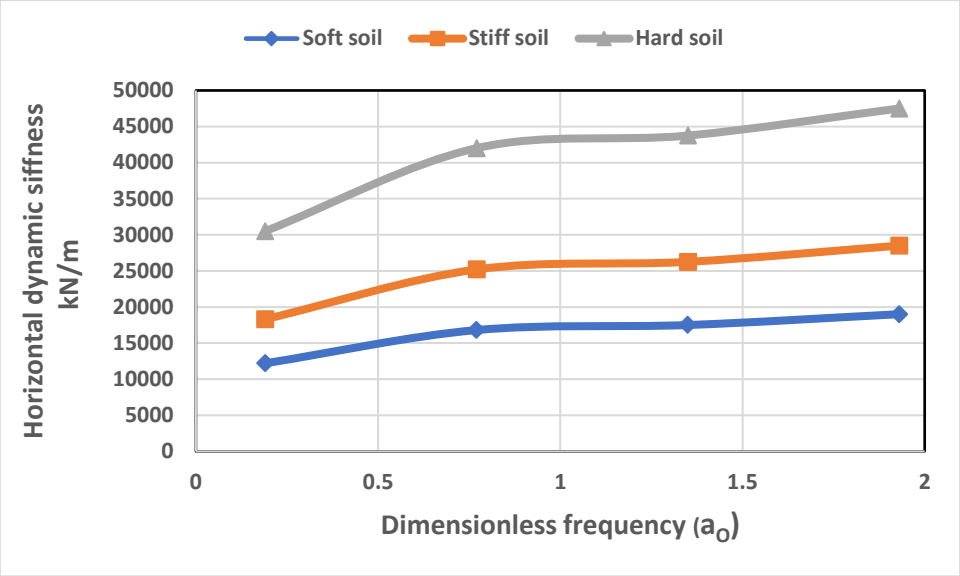

Fig. 7 Dimensionless Frequency (a_o) Versus Horizontal Dynamic Stiffness for the Soil under the Base of the Retaining Wall.

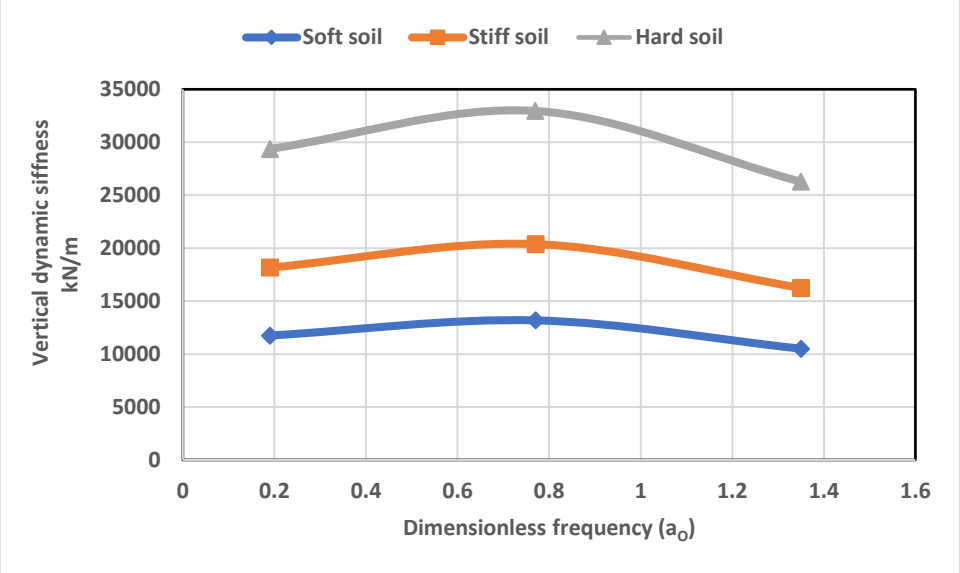

Fig. 8 Dimensionless Frequency (a_o) Versus Vertical Dynamic Stiffness for the Soil under the Base of the Retaining Wall.

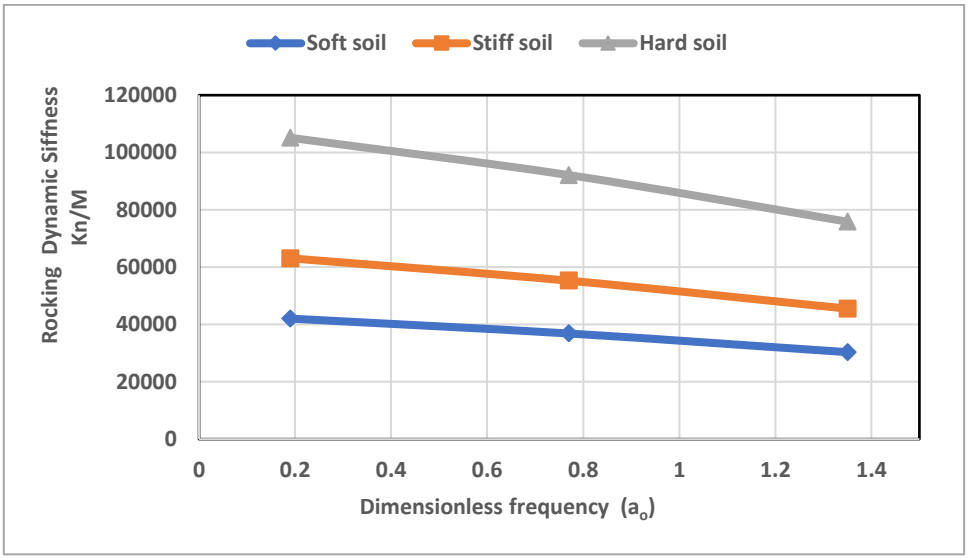

Fig. 9 Dimensionless Frequency (a_o) Versus Rocking Dynamic Stiffness for the Soil under the Base of the Retaining Wall.

Figures 10-12 show the variation of vertical, horizontal, and rocking dynamic damping with dimensionless frequency (a_o) for soft, stiff, and hard soils, respectively. As mentioned above, for dynamic stiffnesses, the dynamic damping for the base under the retaining wall increased with soil hardness. Vertical and horizontal dynamic damping decreased with increasing the dimensionless frequency (a_o), and the rate of decrement decreased with a high value of (a_o). On the other hand, the dynamic rocking increased with (ao). The rate of increment decreased with a high value of (ao). These behaviors are due to the variation in the dimensionless damping coefficient in vertical, horizontal, and rocking, as seen in Figs. 4-6, respectively, meaning that the vertical and horizontal dynamic damping occurred at low values of (a_o) or (ω), while at high values of (a_o) and (ω)for rocking dynamic damping and for all types of soils (soft, stiff, and hard).

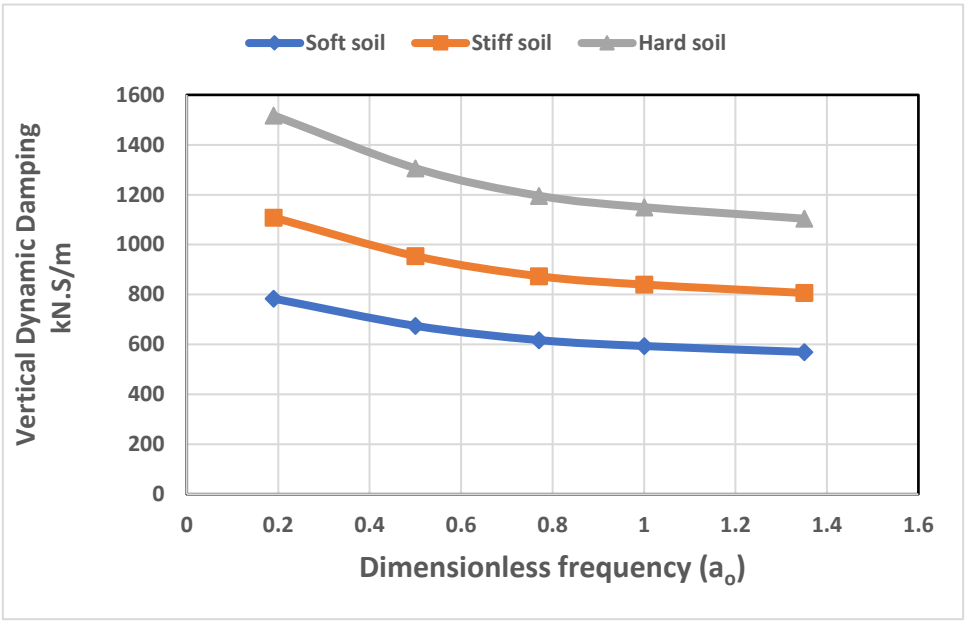

Fig. 10 Dimensionless Frequency (a_o) Versus Vertical Dynamic Damping for the Soil under the Base of the Retaining Wall.

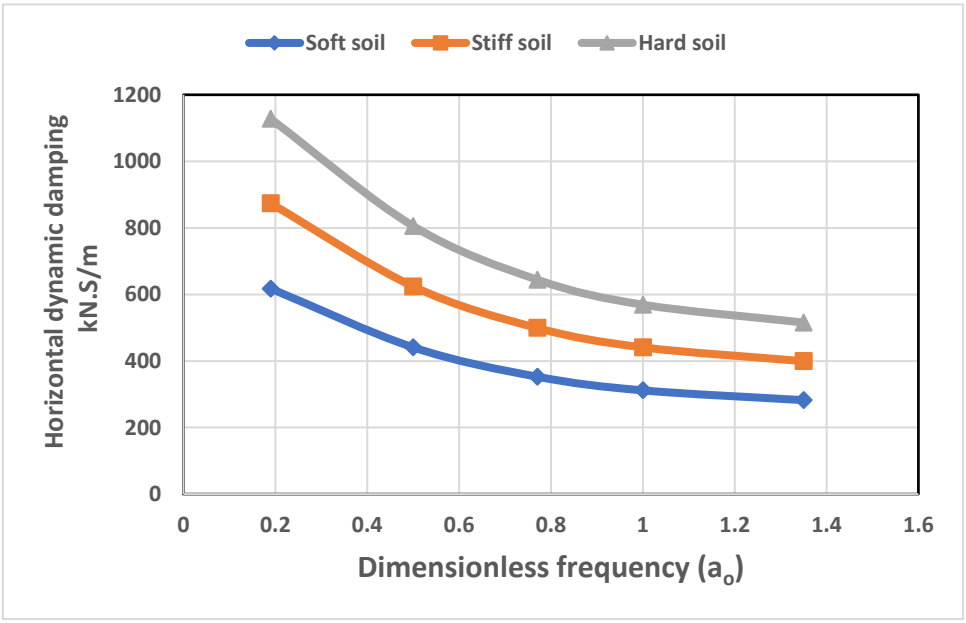

Fig. 11 Dimensionless Frequency (a_o) Versus Horizontal Dynamic Damping for the Soil under the Base of the Retaining Wall.

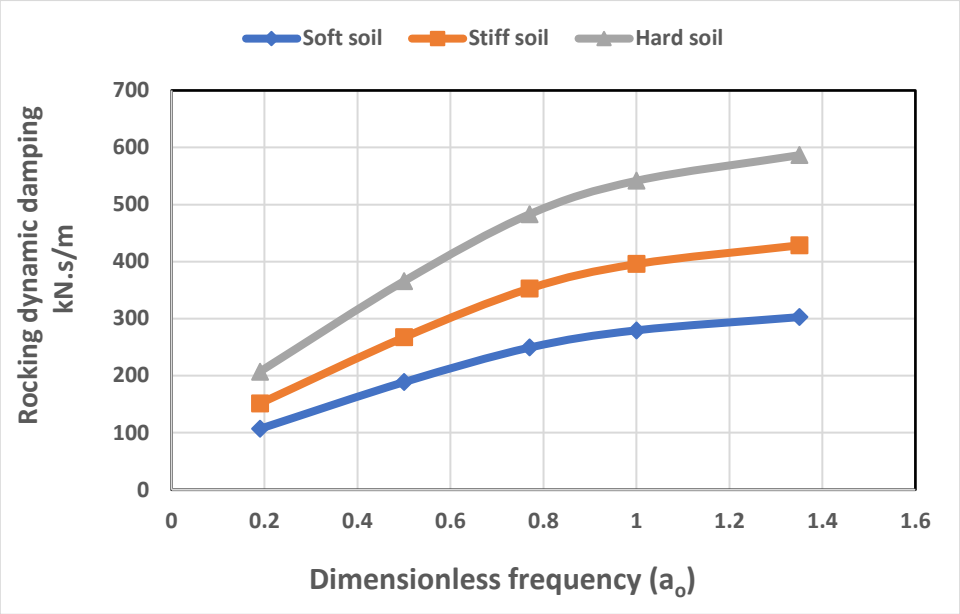

Fig. 12 Dimensionless Frequency (a_o) Versus Rocking Dynamic Damping for the Soil under the Base of the Retaining Wall.

Values of dynamic stiffness have been also estimated for backfill behind the retaining wall. In this case, each of the active and passive dynamic stiffness were evaluated. Figures 13-16 show the effect of the retaining wall height (H) and dimensionless frequency (a_o) on the dynamic active sliding, passive sliding, active rocking, and passive rocking stiffness, respectively. It can also be seen that, as mentioned previously, the shapes of these curves follow the behavior of the stiffness parameters. Generally, all values of stiffness increased with the retaining wall height (H). The maximum value of active dynamic sliding stiffness occurred at the intermediate value of dimensionless frequency (a_o). On the contrary, the maximum value of passive dynamic sliding stiffness occurred at a high value of dimensionless frequency (a_o). Maximum active and passive dynamic rocking stiffness occurred at a low value of (a_o). Furthermore, these curves demonstrated a constant rate of decrement with increasing of (ao), as seen in Figs. 15 and 16.

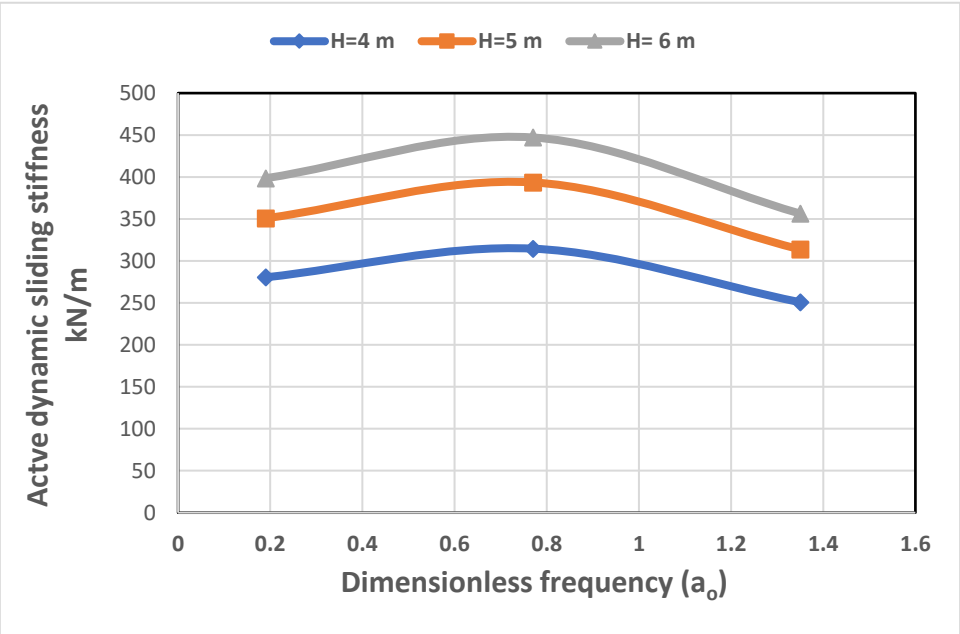

Fig. 13 Dimensionless Frequency (a_o) Verses Active Dynamic Sliding Stiffness for Backfill.

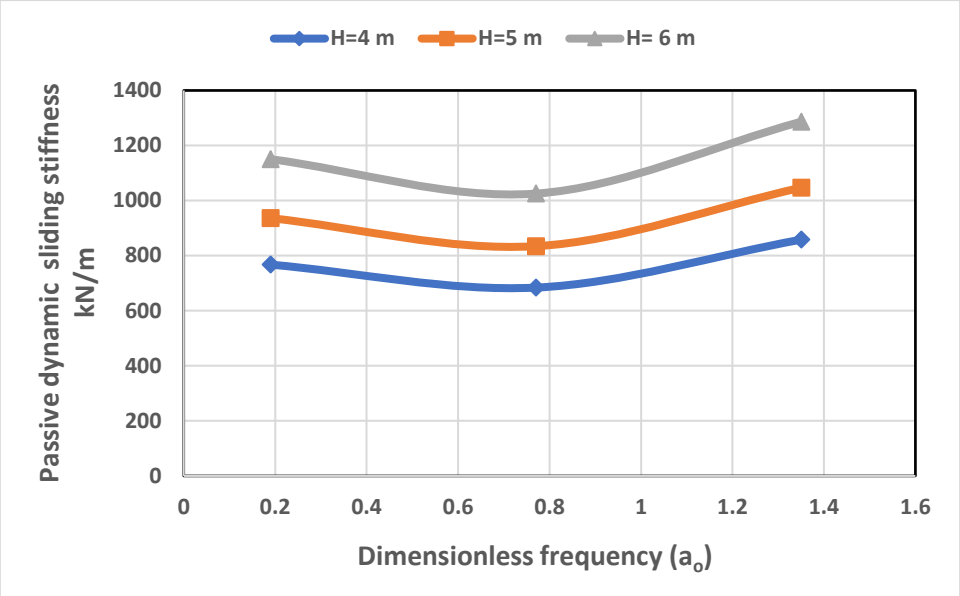

Fig. 14 Dimensionless Frequency (a_o) Verses Passive Dynamic Sliding Stiffness for Backfill.

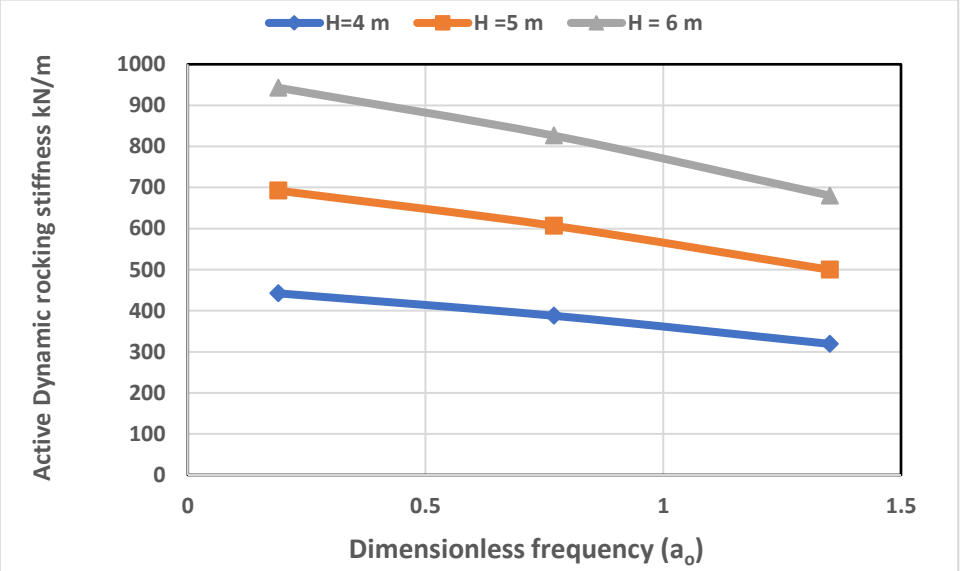

Fig. 15 Dimensionless Frequency (a_o) Verses Active Dynamic Rocking Stiffness for Backfill.

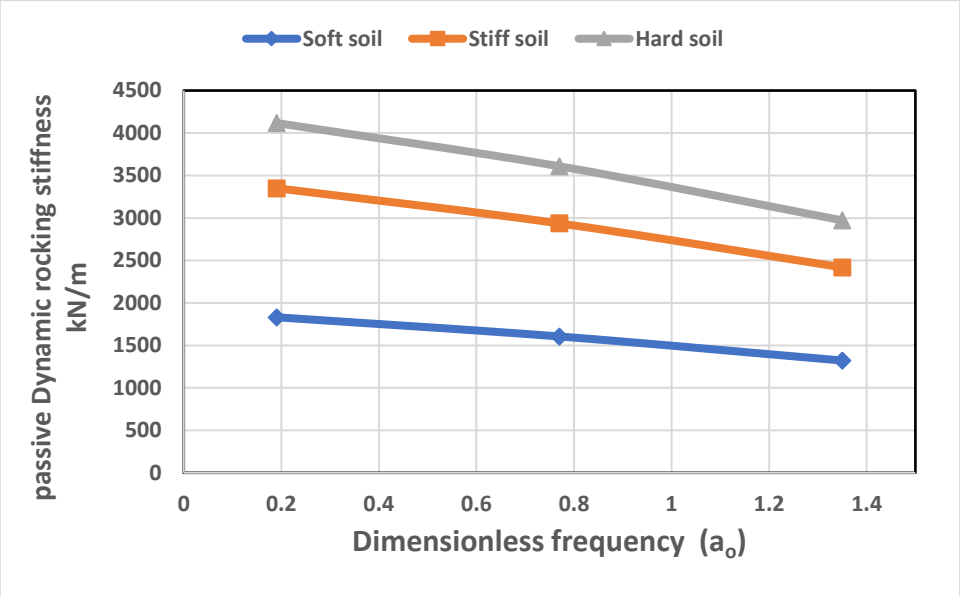

Fig. 16 Dimensionless Frequency (a_o) Verses Passive Dynamic Rocking Stiffness for Backfill.

Evaluating the dynamic sliding and rocking damping for the backfill of the retaining wall are illustrated in Figs. 17 and 18. The values of dynamic sliding damping decreased with increasing dimensionless frequency (a_o), while dynamic rocking damping increased, according to the horizontal damping and rocking damping parameters for both of them. The dynamic sliding damping increased with the height of the retaining wall (H). It should be noticed that there is only one curve in Fig. 18 since the value of dynamic rocking damping of backfill is independent of the height of the retaining wall (H), relating to Eq. (27), which does not contain the height of the retaining wall (H).

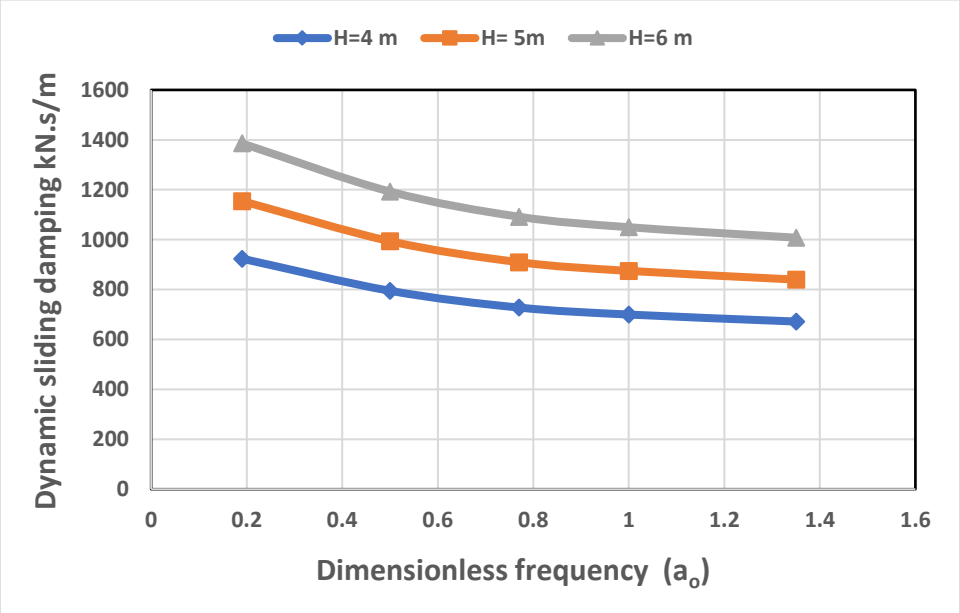

Fig. 17 Dimensionless Frequency (a_o) Verses Dynamic Sliding Damping for Backfill.

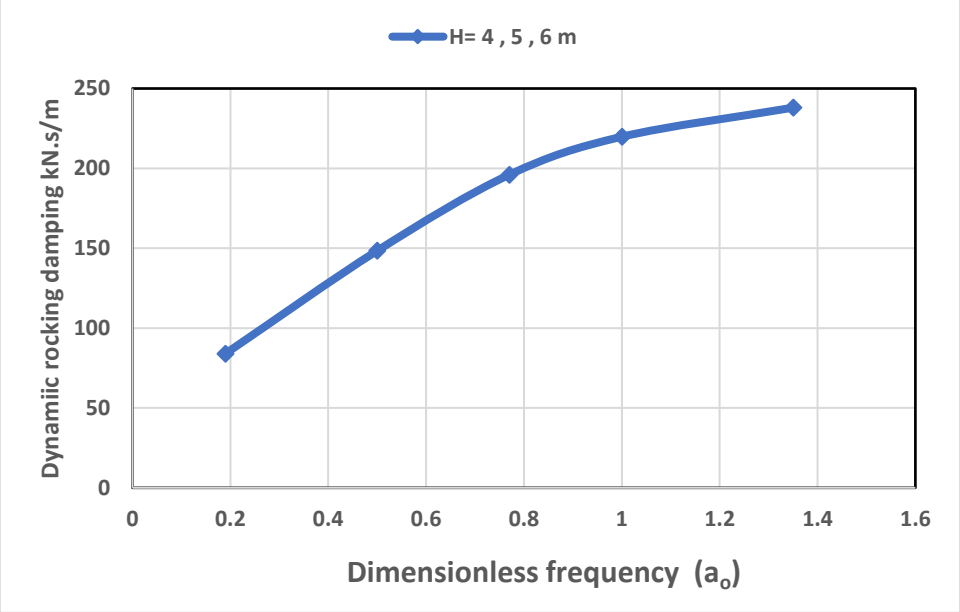

Fig. 18 Dimensionless Frequency (a_o) Verses Dynamic Rocking Damping for Backfill.

6.CONCLUSIONS

Based on the results of the study of dynamic stiffness and damping of rigid retaining walls under seismic loading, the following conclusion can be pointed:

1- The dynamic stiffness and damping of the soil under the base of the retaining wall increased with a shear modulus of the soil (G).
2- The maximum horizontal, vertical, and rocking dynamic stiffness occurred at high, low, and intermediate values of dimensionless frequency (a_o), respectively, in other words, at high, low, and intermediate values of angular frequency (ω).
3- The vertical and horizontal dynamic damping of the soil under the base of the retaining wall occurred at a low value of (a_o) or (ω), while the dynamic rocking

damping occurred at a high value of (a_o) or (ω).

4- The dynamic stiffness and damping of the backfill soil behind the retaining wall increased with the height of the wall. Generally, the increment percentage ranged between (42.1 – 113.2)% when the retaining wall height increased from (4 to 6) m.

5- Active and passive dynamic rocking stiffness of the backfill soil occurred at low values of (a_o) or (ω).

6- The values of dynamic sliding damping and dynamic rocking damping of the backfill soil decreased and increased with increasing (a_o) or (ω), respectively. The percentages of decrement and increment were (37.5)% and (183.3)% when (a_o) increased from (0.19) to (1.35), respectively.

ACKNOWLEDGEMENT

The authors are grateful to the Civil Engineering Department at Mosul University for supporting this research.

REFERENCES

[1] Xiaoyu G, Gopal SP. **Numerical Modelling of Structures Adjacent Retaining Walls Subjected to Earthquake Loading.** *Geosciences* 2020; **10**(12):486.

[2] Rafnsson EA, Prakash S. **Stiffness and Damping Parameters for Dynamic Analysis of Retaining Wall.** *Second International Conference*, St. Louis, Missouri, 1991 Mar 11-15; 1943-1951.

[3] Yadav P, Singh DK, Dahale PP, Padade AH. **Analysis of Retaining Wall in Static and Seismic Condition with Inclusion of Geofoam Using Plaxis 2D.** *Indian Geotechnical Conference*, Bengaluru, India, 2018 Dec 13-15; 1-8.

[4] Chowdhury I, Dasgupta SP. **Earthquake Analysis and Design of Industrial Structures and Infra-structures.** Cham, Switzerland: Springer; 2019.

[5] Gazetas G. **Formulas and Charts for Impedances of Surface and Embedded Foundation.** *Journal of Geotechnical Engineering* 1991; **117**(9):1363-1381.

[6] Mita A, Luco JE. **Impedance Functions and Input Motions for Embedded Square Foundations.** *Journal of Geotechnical Engineering* 1989; **115**(4):491-503.

[7] Bertha O, Jose MJ, Guillermo M. **Radiation Damping for Rigid Foundations: Approximate Expressions.** *Vibro Engineering Procedia* 2019; **27**:103-108.

[8] Veletsos A. **Lateral and Rocking Vibration of Footings.** *Journal of the Soil Mechanics and Foundations Division* 1971; **97**(9):1227-1248.

[9] Veletsos A. **Vibration of Viscoelastic Foundations.** *Earthquake Engineering and Structural Dynamics* 1973; **2**(1):87-102.

[10] Dobry R, Gazetas G. **Dynamic Response of Arbitrarily Shaped Foundation: Experimental Verification.** *Journal of Geotechnical Engineering* 1986; **112**(2):109-135.

[11] Bowles JE. **Foundation Analysis and Design.** 5th ed. New York: McGraw-Hill Companies; 2001.

[12] Gazetas G, Tassoulas JL. **Horizontal Stiffness of Arbitrarily Shaped Embedded Foundation.** *Journal of Geotechnical Engineering* 1987; **113**(5): 440-457.

[13] Gazetas G, Tassoulas JL. **Horizontal Damping of Arbitrarily-Shaped Embedded Foundations.** *Journal of Geotechnical Engineering* 1987; **113**(5): 458-475.

[14] Das BM, Ramana GV. **Principles of Soil Dynamics.** 3rd ed. USA: Engineering Publisher; 2017.

[15] Nandakumaran P. **Behavior of Retaining Wall Under Dynamic Loads.** Ph.D. Thesis. Roorkee, India: Indian Institute of Technology Roorkee; 1973.

[16] Burt GL. **Handbook of Geotechnical Investigation and Design Tables and Franci.** 2nd ed. London, UK: CRC Press; 2017.